Electrochimica Acta 55 (2010) 6358–6366

Contents lists available at ScienceDirect

Electrochimica Acta

journal homepage: www.elsevier.com/locate/electacta

Interaction between myoglobin and hyaluronic acid in layer-by-layer structures—An electrochemical study

Madalina M. Barsan[1], Edilson M. Pinto[1], Christopher M.A. Brett*,[1]

Departamento de Química, Faculdade de Ciências e Tecnologia, Universidade de Coimbra, 3004-535 Coimbra, Portugal

ARTICLE INFO

Article history:
Received 5 May 2010
Received in revised form 12 June 2010
Accepted 18 June 2010
Available online 25 June 2010

Keywords:
Layer-by-layer
Hyaluronic acid
Myoglobin
Redox protein
Electroactive thin film

ABSTRACT

The layer-by-layer (LBL) self-assembled film construction of the biocompatible polymer hyaluronic acid (HA) and single heme redox protein, myoglobin (Mb) is described. The films were built upon gold electrode substrates, both gold quartz crystal electrodes and bulk gold (Au(bulk)) electrodes, and formation of the LBL films was gravimetrically monitored by an electrochemical quartz crystal microbalance. The electrochemical properties of the hyaluronic acid/myoglobin films ($\{HA/Mb\}_n$) were investigated after each deposition step using cyclic voltammetry (CV) and electrochemical impedance spectroscopy (EIS). The CV response presented an oxidation peak at +0.3 V *vs.* SCE, not characteristic of the redox protein myoglobin, and, the peak current decreased slightly with each additional bilayer. CV at Au(bulk) electrodes in pH 5.0 acetate buffer solution, containing Mb, presented the same oxidation peak as observed at $\{HA/Mb\}_n$ modified electrodes, confirming the presence of the same electroactive species. The Mb oxidation peak current depends linearly on scan rate, characteristic of adsorbed thin-layer electrochemical systems, attributed to free adsorbed heme. Impedance spectra, recorded after deposition of each bilayer, were in agreement with the cyclic voltammetry observations.

1. Introduction

The immobilization of redox proteins on electrodes is a topic of active research both for obtaining a better understanding of enzyme catalysis [1] and for the development of biosensors [2,3]. The study of the direct electron transfer of proteins immobilized on solid electrodes can provide information about the electron transfer between enzymes and proteins in real biological systems, in this way enabling the preparation of a new type of third generation biosensor, bioreactor and biomedical device, without the use of mediators [4].

Various methods and approaches for protein immobilization have been developed. Among the techniques that enable a high control of both chemistry and spatial order on the surface, self-assembled monolayers (SAMs) and Langmuir–Blodgett techniques have been the most commonly used [5]. A novel method for the build-up of multilayered polyelectrolyte films is the layer-by-layer (LBL) technique [6], which consists in the alternate adsorption on solid substrates of oppositely charged species from appropriate solutions, through electrostatic interaction [7]. One of the many attractive features of LBL self-assembly is the remarkable nanoscale control that can be exercised over the properties of the film (e.g. thickness, roughness, wettability and swelling behaviour), by varying the conditions used to assemble the film, such as pH, ionic strength, polymer functionality and polymer concentration [8,9].

Layer-by-layer films can be used for immobilizing and carrying out direct electrochemistry of redox enzymes or proteins. Among proteins, heme proteins, metalloproteins containing the heme prosthetic group, either covalently or non-covalently bound to the protein, have been extensively studied, due to their capacity to undergo reduction and oxidation at the iron heme [2]. Some of these proteins are electron carriers (cytochrome *c*, catalase), others are involved in catalysis (e.g. peroxidase, cytochrome *c* oxidase) and in active membrane transport or in oxygen transport (e.g. hemoglobin, myoglobin, cytoglobin) [10]. Myoglobin is a monomeric single heme protein (see Fig. 1(A) for heme chemical structure), relatively small (Mr 16,700) found mainly in muscle tissue where it serves as an intracellular storage site for oxygen and facilitates oxygen diffusion in rapidly contracting muscle tissue [10]. Both myoglobin and hemoglobin immobilized in different LBL films fabricated on electrode surfaces, exhibit direct and reversible cyclic voltammetric responses of their heme Fe(II)/Fe(III) redox couple [2,7,11–14].

* Corresponding author. Tel.: +351 239 835295; fax: +351 239 827703.
E-mail addresses: brett@ci.uc.pt, cbrett@ci.uc.pt (C.M.A. Brett).
[1] ISE member.

0013-4686/$ – see front matter © 2010 Elsevier Ltd. All rights reserved.
doi:10.1016/j.electacta.2010.06.058

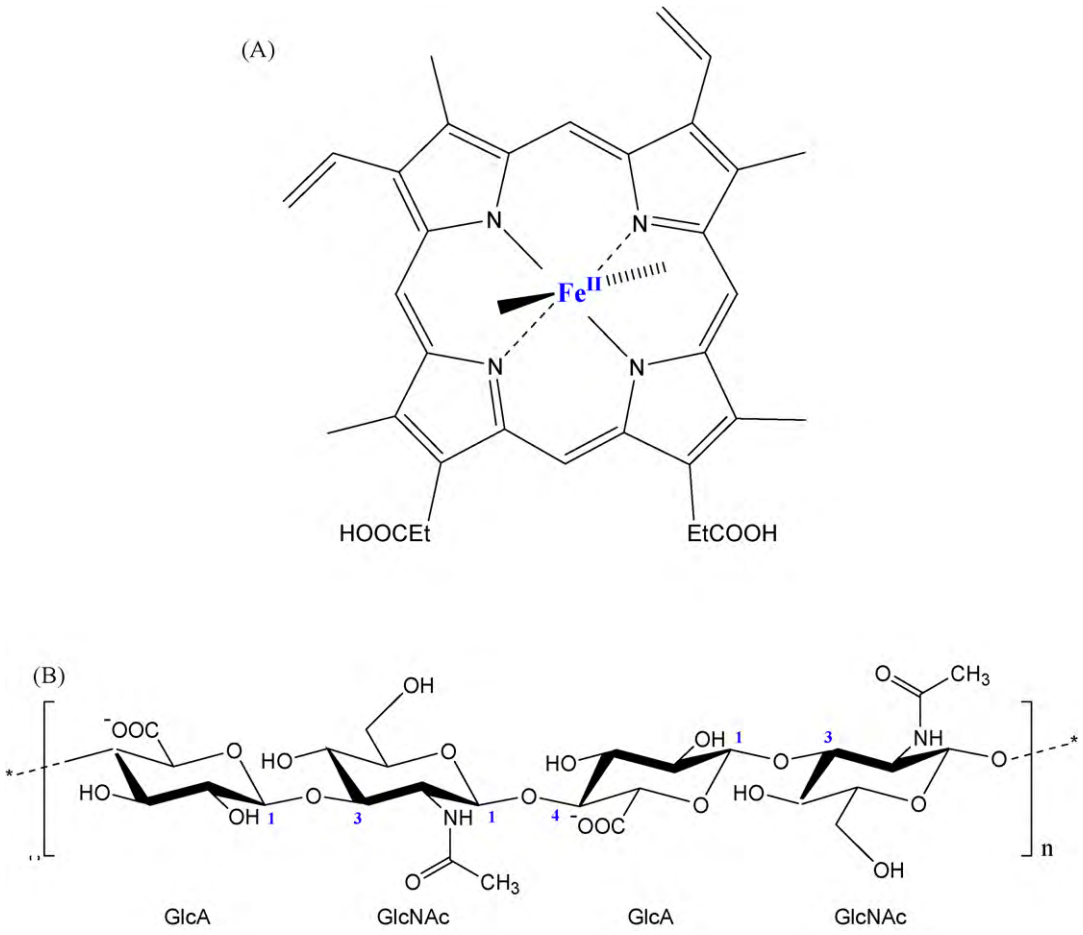

Fig. 1. Chemical structure of (A) heme in myoglobin and (B) hyaluronic acid (HA).

The multilayer technique has been mainly applied to synthetic polyelectrolytes [15], but in recent years it has been extended to biopolymers, many of which are polysaccharides, among them is hyaluronic acid. HA (hyaluronate at physiological pH) is a linear polysaccharide chain with an average molar mass ranging from 10^4 to 10^7 Da [16]. It is a natural non-sulfated glycosaminoglycan (GAG) consisting of linear poly-anionic polymer chains of alternating *N*-acetyl-D-glucosamine and β-D-glucuronic acid residues linked through 1–3 and 1–4 respectively (see Fig. 1(B)). It is highly hydrophilic due to the presence of hydroxyl and carboxyl groups and, unusually for a GAG, does not bind to a protein core. Despite its hydrophilicity, HA is a weak polyacid with a very low charge density because only one charge is present for each repeating disaccharide unit [17]. Hyaluronates form clear, highly viscous solutions that serve as lubricants in the synovial fluid of joints and give the vitreous humour of the vertebrate eye its jelly-like consistency (the Greek *hyalos* means "glass"; hyaluronates can have a glassy or translucent appearance). Hyaluronate is also an essential component of the extracellular matrix of cartilage and tendons, to which it contributes tensile strength and elasticity as a result of its strong interactions with other components of the matrix [10]. Many of the physiological and cell biological functions of HA are based on its specific interactions with matrix proteins or cell surface HA-receptor proteins [18]. Owing to these properties, HA has been extensively used in LBL assemblies, mostly together with poly(allylamine) (PAA) [19] or polylysine (PLL) [9,20], forming self-assembled films, which were also applied for drug delivery capsule preparation [21–23]. HA/chitosan films have also been prepared on various surfaces [24] and the loading behaviour of these films toward Mb was studied by Lu and Hu [25]. The same authors reported on $\{HA/Mb\}_n$ film formation on pyrolytic graphite and observed direct electrochemistry of the protein and that an increase in salt concentration of the supporting electrolyte enhanced the amount of electroactive Mb [26].

In protein-modified electrodes it is important to consider that the protein immobilization method can sometimes affect their conformation (secondary and tertiary structure) and then the protein's properties, so it is necessary to ascertain whether the observed coverage, redox properties and electron transfer behaviour are typical for the protein under study. In recent work, de Groot et al. reported on heme release from myoglobin (Mb) immobilized in films of didodecyl dimethyl ammonium bromide (DDAB) [27,28] and in layer-by-layer assemblies of Mb with polystyrene sulfonate, both on pyrolytic graphite [29].

In the present work we investigate layer-by-layer assemblies of electroactive myoglobin and the poly-anionic polymer hyaluronic acid on Au-coated piezoelectric crystals for the quartz crystal microbalance (QCM) and on Au-bulk electrodes. The interest is to explore how proteins interact with the well-known, biocompatible hyaluronic acid, and to observe how the native bioactivity of the protein is preserved in such layer-by-layer protein/HA structures. This will enable application of this immobilization method or to use this protein/HA structure to immobilize other biomolecules, such as enzymes, with the advantage of being a simple technique, in which only a very small amount of the biomolecule is used. With this aim, the build-up mechanism of $\{HA/Mb\}_n$ layers and the characteristics of the films obtained have been investigated using cyclic voltammetry (CV) as well as gravimetrically using the electrochemical quartz

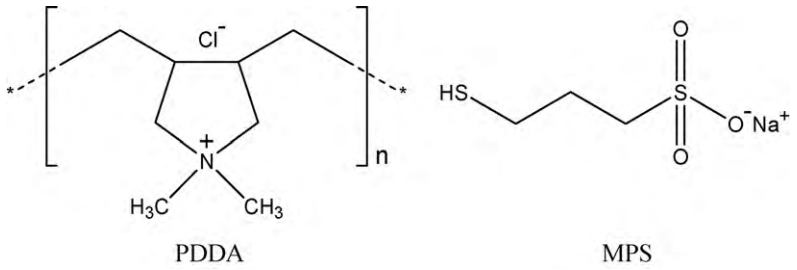

Fig. 2. Chemical structures of poly(diallyl dimethyl ammonium chloride) (PDDA) and 3-mercapto-1-propanesulfonate (MPS).

crystal microbalance (EQCM), and by electrochemical impedance spectroscopy (EIS). Results obtained from the different techniques are compared in order to elucidate whether the observed electrochemical response of the $\{HA/Mb\}_n$ assemblies is due to the native protein or to a partially or completely denatured protein.

2. Experimental

2.1. Chemicals

All chemicals were analytical grade and used as received, without further purification. Solutions were prepared with Millipore Milli-Q nanopure water (resistivity ≥18 MΩ cm).

Sodium 3-mercapto-1-propanesulfonate (MPS) (technical grade 90%) and poly(diallyl dimethyl ammonium chloride) PDDA (see Fig. 2 for chemical structures), very low molecular weight 35% wt. in water were from Aldrich, Germany. Myoglobin Mb, from horse heart (minimum purity 90%, iron content minimum 0.2%) and sodium phosphate dibasic heptahydrate were from Sigma, Germany and hyaluronic acid sodium salt, from *Streptococcus equi* sp. was from Fluka, Germany. Sodium acetate, acetic acid and sodium dihydrogen phosphate were from Riedel-deHaën, Germany; disodium tetraborate from Analar, England and boric acid from May & Baker Ltd, Dagenham, England. Potassium bromate was from Merck, Germany.

Buffer solutions were prepared as shown in Table 1.

Experiments were performed at room temperature (25 ± 1 °C).

2.2. Film assembly

For the preparation of the $\{HA/Mb\}_n$ films, gold crystal electrodes (AuQCM) and Au-bulk electrodes were used as substrate. The 6 MHz AuQCM of 0.28 cm^2 exposed geometric area were provided by KVG-Germany. The Au-bulk disk electrode of 0.10 cm diameter was from Cypress System, USA and made with high purity (>99.9%) Au.

Au electrodes were first immersed in freshly prepared piranha solution (3:1 H_2SO_4 95–97%:7 M H_2O_2) for at least 10 min and then rinsed with water and dried in N_2 stream. The cleaned electrodes were then left from one day to another in 4 mM MPS solution (MPS dissolved in 1:1 ethanol:0.01 M H_2SO_4), to negatively charge the Au surface by the chemical adsorption of an MPS monolayer, through Au–S covalent bonds. The other precursor, positively charged PDDA, was then adsorbed by immersing the AuQCM-MPS(−) in 3 mg ml^{-1} PDDA in 0.05 M NaAcBS pH 5.0 solution, during 20 min. In this way, before starting $\{HA/Mb\}_n$ LBL deposition, the electrode substrate is positively charged: AuQCM-MPS(−)/PDDA(+). The layer-by-layer assembly of HA and Mb was carried out by alternately immersing the electrodes, during 20 min, in 1 mg ml^{-1} HA and 1 mg ml^{-1} Mb (both prepared in 0.05 M NaAcBS pH 5.0 buffer solution). Before each immersion of electrodes in the solutions containing HA or Mb, they were rinsed with water and dried in a nitrogen stream for about 1–2 min. The build-up process was carried out until a desired number of bilayers $\{HA/Mb\}_n$ were deposited on the Au electrode substrates.

2.3. Apparatus

A three-electrode electrochemical cell was used, containing the AuQCM or Au(bulk) modified electrodes as working electrode, a platinum foil counter electrode and a saturated calomel electrode (SCE) as reference.

Electrochemical measurements were performed using a computer-controlled μ-Autolab Type II potentiostat–galvanostat running with GPES (general purpose electrochemical system) for Windows version 4.9 software (Metrohm-Autolab, Utrecht, Netherlands).

The electrochemical impedance measurements were carried out on a PC-controlled Solartron 1250 Frequency Response Analyzer, coupled to a Solartron 1286 Electrochemical Interface using ZPlot 2.4 software (Solartron Analytical, UK). A rms perturbation of 10 mV was applied over the frequency range 65.5 kHz–0.01 Hz, with 10 frequency values per decade. The spectra were recorded at the open circuit potential (OCP), measured immediately prior to each EIS experiment.

Gravimetric studies were performed using a homemade electrochemical quartz crystal microbalance (EQCM) connected to a μ-Autolab (Metrohm-Autolab, Utrecht, Netherlands), controlled by GPES Autolab software.

The pH-measurements were made with a CRISON 2001 micro pH-meter (Crison, Spain) at room temperature.

3. Results and discussion

3.1. $\{HA/MB\}_n$ layer-by-layer film assembly monitored by QCM

The QCM was used to monitor the assembly of $\{HA/MB\}_n$ layer-by-layer films in situ. The mass variation in time (Δm) is directly related to the induced frequency variation (Δf), by the Sauerbrey equation, for rigid films adsorbed at the QCM crystal surface [30].

Table 1
Preparation of buffer solutions.

Buffer solution	Composition	pH
0.05 M sodium acetate saline (NaAcBS)	0.05 M ($CH_3COONa + CH_3COOH$) + 0.1 M KBr	4.0, 4.7, 5.0, 5.3, 5.7
0.05 M sodium phosphate saline (NaPBS)	0.05 M ($NaH_2PO_4 + Na_2HPO_4 \cdot 7H_2O$) + 0.05 M KBr	5.7, 7.0
0.05 M sodium tetraborate saline (NaBBS)	0.05 M ($Na_2B_4O_7 \cdot 10H_2O + B(OH)_3$) + 0.1 M $KBrO_3$	9.0

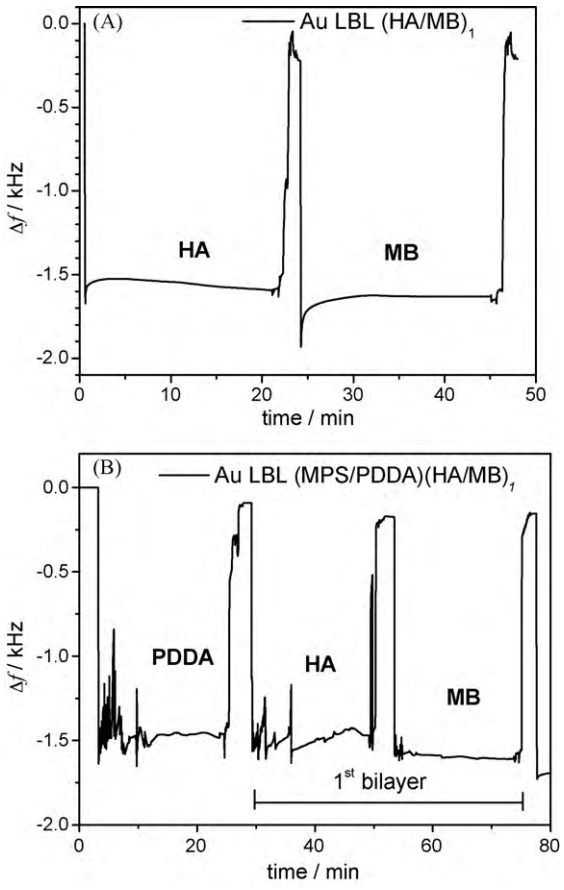

Fig. 3. (A) Frequency shift during the deposition of HA and Mb monolayers at AuQCM electrodes and (B) typical deposition profile for the first 3 monolayers: PDDA(+) and $\{HA/Mb\}_1$.

The relationship between the mass frequency and the induced mass variation, for the present system is:

$$\Delta f = -2.91 \times 10^8 \Delta m \quad (1)$$

expressing f in Hz and m in g.

A typical frequency shift during each monolayer deposition is presented in Fig. 3(A). As observed, the frequency values decrease after immersion of the crystal in HA or Mb solution, as a result of mass adsorption at the AuQCM surface. The frequency peaks that appear in Fig. 3 are due to the oscillation of the crystal in air, between its immersions in the desired solution.

Fig. 3(B) shows formation of the first 3 monolayers containing the precursor PDDA(+) and the first bilayer $\{HA/Mb\}_1$. The deposition of the first layers is not uniform, and is highly influenced by the formation of microstructures (islands) adsorbed at the surface [20], a hypothesis which is supported by cyclic voltammetry results, see in Section 3.2.2.

The $\{HA/Mb\}_n$ film grows in an irregular manner, and the amount of HA and Mb adsorbed after each monolayer deposition was rather different. The overall shift in frequency up to the sixth bilayer is ≈1.5 kHz, corresponding to a deposited film of ∼5.0 μg, with an average of ∼0.83 μg for each {HA/Mb} bilayer.

3.2. Cyclic voltammetry

Interaction between the electrode and the protein should be sufficient for immobilization but should not significantly affect the structure of the enzyme and its functionality. Even though there is evidence of efficient myoglobin immobilization in layer-by-layer structures, without altering its properties and with direct electrochemistry occurring between the electrode and the protein [7,14,26,31], there are reports regarding heme release in LBL assemblies [27–29]. The cyclic voltammetric study was carried out taking into account the possibility of heme release, as well as or instead of direct electrochemistry of myoglobin [26], and can be seen in Figs. 4–8.

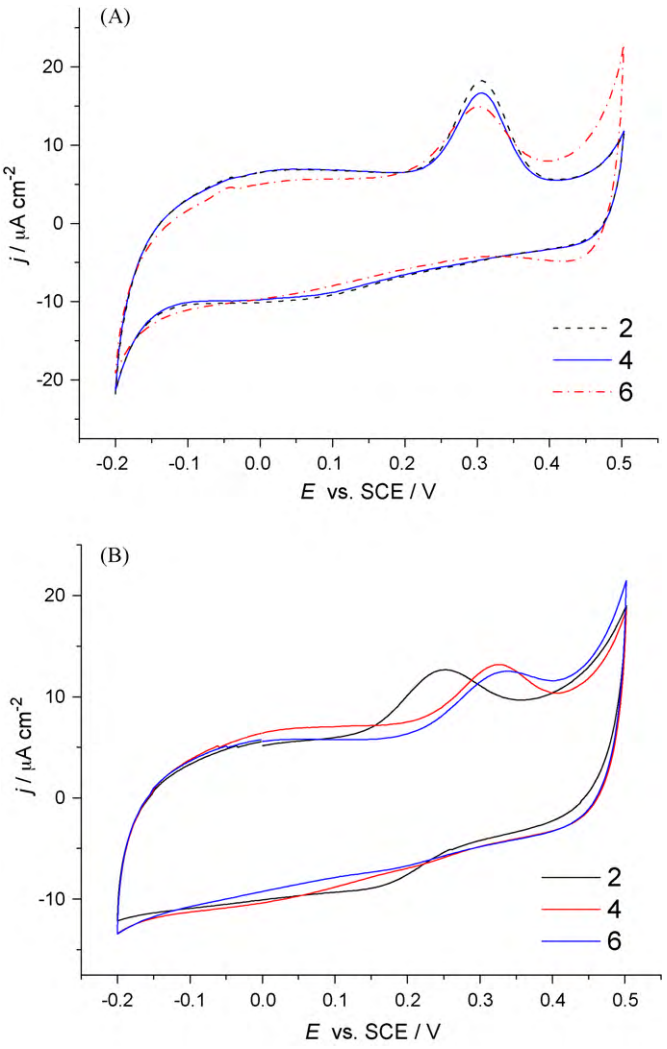

Fig. 4. Cyclic voltammograms in 0.05 M NaAcBS pH 5.0 at (A) AuQCM- and (B) Au(bulk)-MPS(−)/PDDA(+)/$\{HA/Mb\}_n$ where n = 2, 4 and 6; scan rate = 50 mV s^{-1}.

3.2.1. Possible heme release in $\{HA/Mb\}_n$ layer-by-layer structures

Figs. 4–6 show cyclic voltammetric results from which the possibility of heme release can be assessed. Several facts support its occurrence:

(I) The cyclic voltammetric response recorded during film formation at AuQCM-MPS(−)/PDDA(+)/$\{HA/Mb\}_n$, where n = 2, 4 and 6 (see Fig. 4(A) and (B)) is not a typical response for Mb in LBL systems. First, the formal potential $E^{0\prime}$ of Mb is reported to be ∼−0.34 V *vs.* SCE in phosphate buffer pH 7.0 solution [7,14,31] and, in our case, the CV has an irreversible oxidation peak at ∼+0.3 V *vs.* SCE, which probably corresponds to oxidation of the free heme, as reported in [29]. Moreover, the oxidation peak does not increase in size with each deposition step, as would be expected and reported in [7,13,14], but slightly

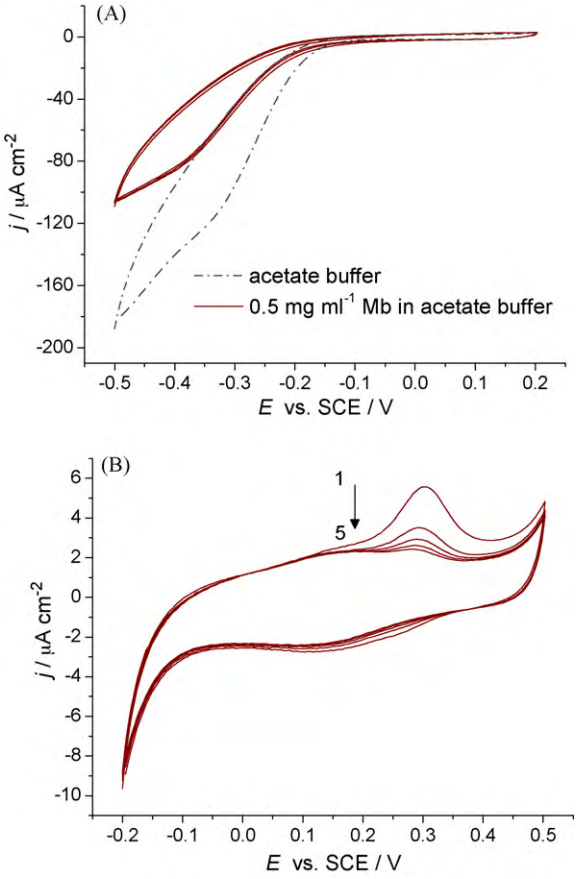

Fig. 5. Cyclic voltammograms at Au(bulk) electrode in 0.05 M NaAcBS pH 5.0 containing 0.5 mg ml^{-1} Mb, at 10 mV s^{-1} between (A) −0.5 and +0.2 V, (B) −0.2 and +0.5 V *vs.* SCE.

decreases. Anyway, it should be considered that in order for electron transfer between the electrode and the redox group of the protein to occur, the distance between them should not be much greater than 1.4 nm, the maximum distance observed between two redox proteins that can transfer electrons in biological systems [32]. Taking this into account, we consider that the oxidation peak is due to oxidation of adsorbed free heme, probably immobilized at the surface during the first 2 bilayers.

(II) In order to examine the electrochemical behaviour of myoglobin in solution, cyclic voltammetry was performed at a bulk Au electrode (Au(bulk)) immersed in acetate buffer pH 5.0 containing 0.5 mg ml^{-1} Mb. In the negative potential region, where the Mb mid-point potential is reported to be, no peaks were recorded (Fig. 5(A)), but in the potential range from −0.2 to +0.5 V *vs.* SCE, an oxidation peak appeared at the same potential as recorded at AuQCM-MPS(−)/PDDA(+)/{HA/Mb}$_n$ electrode (see Fig. 5(B)). In order to elucidate whether the species that gave rise to the oxidation peak is adsorbed on the electrode surface or is in solution, a scan rate study was performed in the same solution containing 0.5 mg ml^{-1} Mb, at different scan rates from 10 upto 100 mV s^{-1}; above this scan rate the waves began to be insufficiently well defined for accurate analysis. It was found that the oxidation peak current depends linearly on scan rate obeying the equation $I_{pa} = 0.04 + 0.11v$ (see Fig. 6, 1(B)), characteristic of adsorbed thin-layer electrochemical systems. The same electrode was then subjected to the same scan rate study in acetate buffer pH 5.0, without any Mb. The electrochemical response recorded (Fig. 6, 2(A)) had the same linear relationship between I_{pa} and v, Fig. 6, 2(B). This demonstrates that the electrochemical response is due to exactly the same species, which is adsorbed at the electrode.

(III) The electrochemical behaviour of free hemin in solution was also tested at Au(bulk) electrodes. For this purpose, a solution of 1 mg mL^{-1} hemin was prepared by dissolving hemin in 0.025 M borate buffer solution, pH 11.4, since hemin is soluble only in highly basic solution. An appropriate amount of this hemin solution was then injected to the 0.5 M + 0.1 M KBr acetate buffer solution pH 5.0, so that the final concentration of hemin was 0.091 mg mL^{-1}. The CV response of the Au(bulk) electrode in the hemin solution is presented in Fig. 7(A). The peaks were very similar to those observed for Mb in solution and Mb adsorbed at the Au(bulk) electrode, suggesting that the same electroactive species, hemin, is responsible for the electrochemical response. The peak current is linearly dependent on the square root of the scan rate, obeying the equations: $I_{pa} = -32.2 + 5.8 \times v^{1/2}$ and $I_{pc} = 31.1 - 5.9 \times v^{1/2}$, indicating that the process is diffusion controlled.

An experiment involving hemin adsorption at Au(bulk) electrodes was also undertaken, by immersing a freshly cleaned electrode in a 0.5 mg mL^{-1} hemin solution (prepared in 0.025 M borate buffer solution, pH 11.4) during 30 min. CV experiments were then done at the modified electrode in the same experimental conditions as for hemin in solution, and are shown in Fig. 7(B). Comparing Fig. 7(A) and (B), the CV peaks are better defined when hemin is in solution, probably because pure hemin does not adsorb easily at Au electrodes. The mid-point potential of the oxidation and reduction peaks of hemin, in solution and adsorbed, is the same, with a lower peak potential separation in the case of adsorbed heme.

(IV) The voltammetric response of AuQCM-MPS(−)/PDDA(+)/{HA/Mb}$_6$ was recorded in acetate buffer pH 5.0 after being immersed for 5 min in 0.05 M NaPBS solution pH 7.0 or in 0.05 M NaBBS solution pH 9.0, both buffers having the pH above the p*I* of Mb (pI_{Mb} = 6.8) [33]. The experiment was carried out to verify if the multilayer system is being destroyed, since the electrostatic interactions between HA (negatively charged since pK_a = 2.9) [16] and Mb which also becomes negatively charged, are not acting anymore. We observed that the brownish color of the Mb/HA modified electrode, which appears due to the overlapping of the Mb layers that absorb visible light, disappears after immersion in pH 7.0 and 9.0 buffers, which sustains the hypothesis that the LBL multilayers are being washed away. The CV recorded, after the electrode was immersed in these buffers, presented the same oxidation peak as recorded before immersion, at the same potential and having the same peak current, demonstrating the existence of electroactive species adsorbed at the electrode surface, other than Mb, and this is probably the released heme.

(V) The storage stability was evaluated by comparing the CV response of an AuQCM-MPS(−)/PDDA(+)/{HA/Mb}$_6$ electrode after keeping it in air, at room temperature. After 40 days of storage the oxidation peak current decreased by only 10% from its initial value, which again suggests that the voltammetric response is given by a species other than the Mb protein, knowing that the protein is expected to be denatured under these conditions.

3.2.2. Comparison between AuQCM- and Au(bulk)-modified electrodes

In order to compare the electrochemical behaviour of both types of modified Au electrode, cyclic voltammograms recorded under different conditions were evaluated simultaneously. During layer-by-layer deposition, the same tendency in peak oxidation decrease

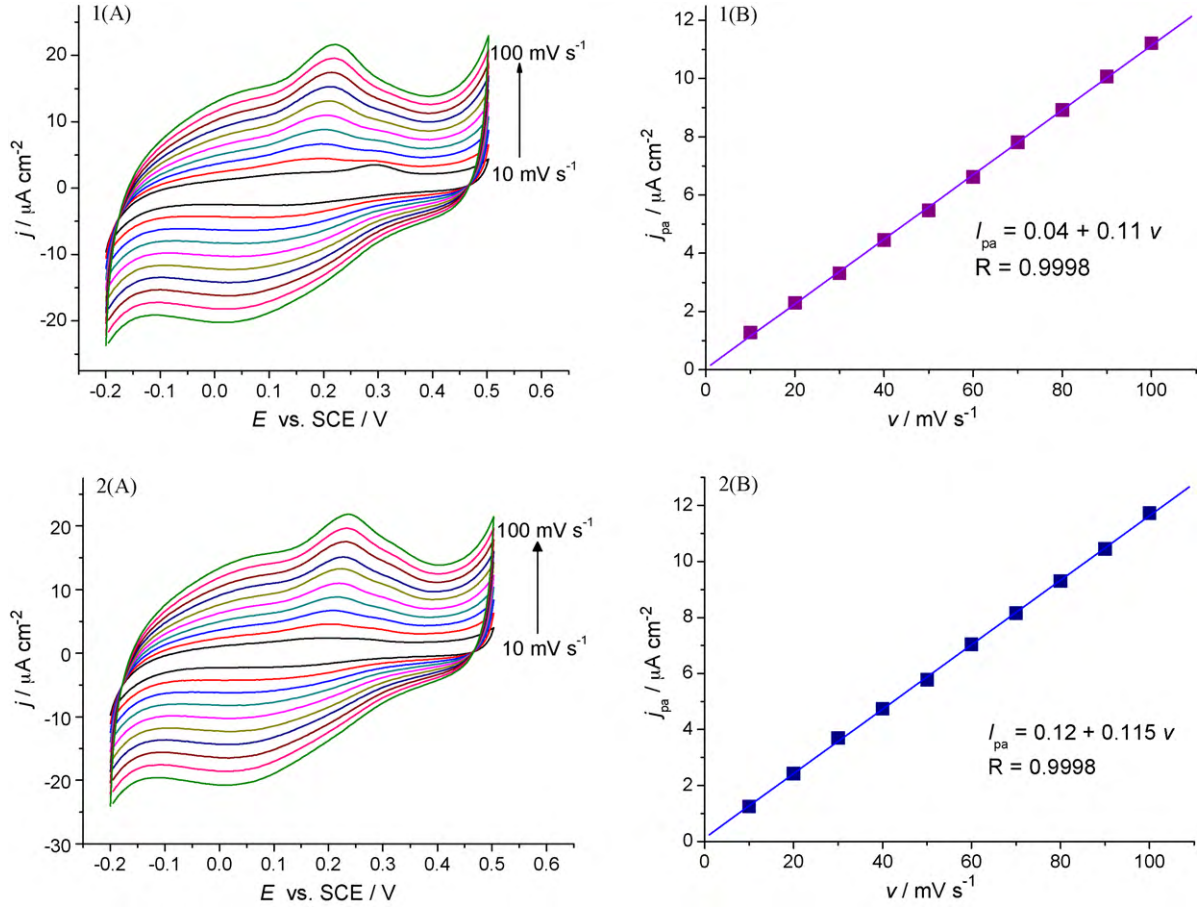

Fig. 6. Cyclic voltammograms at Au(bulk) electrode 1(A) in 0.05 M NaAcBS pH 5.0, containing 0.5 mg ml^{-1} Mb and 2(A) after transferring to 0.05 M NaAcBS. 1(B) and 2(B) are the corresponding plots of j_{pa} *vs.* scan rate.

was observed (see Fig. 4(A) and (B)), which, as already mentioned, occurs because the response is probably due to an adsorbed species, the electron transfer becoming more difficult after each additional layer. Since the differences in peak currents are not very significant, it can be concluded that the overall redox process does not involve the rate-determining diffusion of other additional counterions from the solution, or that their diffusion to the electrode is not influenced by the deposition of each layer.

In the case of the Au(bulk)-MPS(−)/PDDA(+)/{HA/Mb}$_n$ electrode it is observed that during LBL construction, the peak current decreases slightly with each bilayer deposited and the oxidation peak potential is shifted from 250 mV *vs.* SCE, for two bilayers, to more positive potentials of ∼+330 mV *vs.* SCE for 4–6 bilayers.

The same is observed at AuQCM-MPS(−)/PDDA(+)/{HA/Mb}$_n$, the peak current decreasing more with each layer deposition. Also, the oxidation peak potential maintains its value of +305 mV *vs.* SCE during the deposition process.

Other papers describing the reversible electrochemical behaviour of Mb in LBL structures, report an increase of the peak current with the number of bilayers, due to an increase in the amount of electroactive Mb. The fact that in our case, the peak current decreases after each layer deposition is another indicator that it is not Mb itself that is responsible for the electrochemical properties of the {HA/Mb}$_n$ Au modified electrodes, but rather an electroactive species contained by it, that is free to diffuse through the layers to the electrode substrate surface. In this way, the diffusion through the layers becomes more and more difficult with the deposition of new layers.

The fact that the peak potential recorded at Au(bulk)-MPS(−)/PDDA(+)/{HA/Mb}$_2$ has the same value as in the case of the Au(bulk)-Mb(adsorbed) electrode, leads to the conclusion that up to the second deposited bilayer, the LBL films are not homogeneous and there are still unmodified islands on the electrode surface. When the electrode is immersed in the Mb solution, Mb, or species contained by it, can adsorb directly on the unmodified Au electrode surface, the electrode showing the behaviour of one modified only by adsorbed Mb.

The non-uniform, random deposition of the first bilayers was observed also at AuQCM electrodes during the gravimetric experiments. In the case of AuQCM substrate, the LBL structure is formed more readily and covers a larger area of the electrode surface, so the electrochemical behaviour is the same for 2 as for 6 bilayers. The only possible explanation lies in the different morphologies and structures of the two Au electrodes, the more porous structure of the Au thin film deposited on the quartz crystal being more appropriate for this type of LBL construction. Moreover, the peak current measured for the AuQCM 6-bilayer film is much higher than for the Au(bulk) 6-bilayer film (see Fig. 8). This is probably not only because the electroactive species adsorbs better on the AuQCM, but also because the available surface area of the AuQCM electrode is larger, due to its rough surface.

3.2.3. Comparison between Au(bulk)-MPS(−)/PDDA(+)/{HA/Mb}$_6$ and Au(bulk)–Mb(adsorbed)

If CV responses of both modified electrodes are compared (see Figs. 4(B) and 6, 2(A)), the overall profiles are very similar with small differences in the oxidation peak potential and the reduction

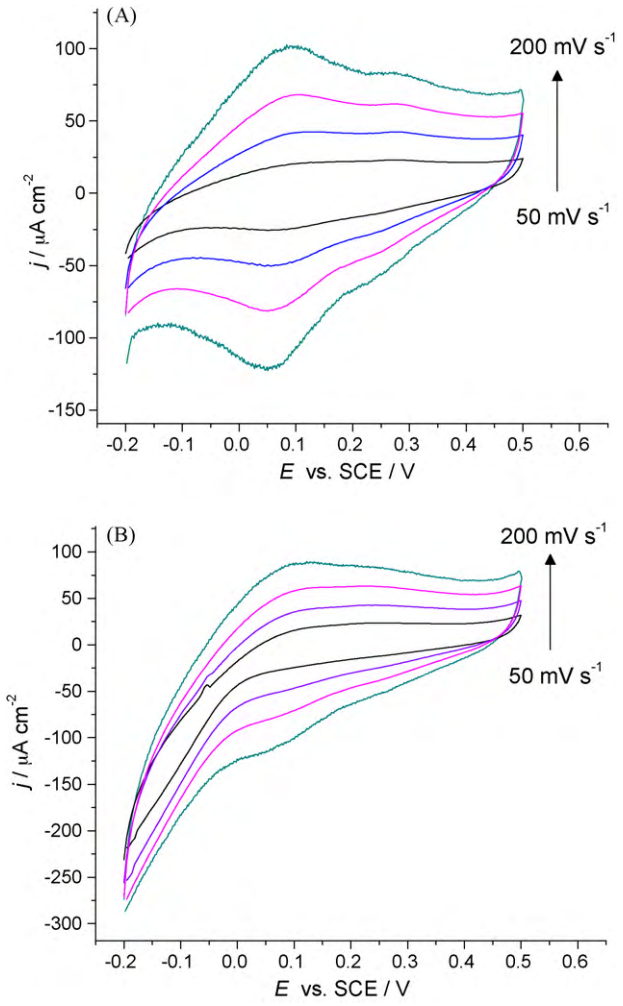

Fig. 7. Cyclic voltammograms recorded at Au(bulk) electrode in 0.05 M + 0.1 M KBr pH 5.0 (A) with 0.1 mg ml^{-1} hemin in solution and (B) after 30 min immersion in 0.5 mg ml^{-1} hemin + 0.025 M borate buffer solution, pH 11.4 for adsorption to occur. Scan rates: 50, 100, 150 and 200 mV s^{-1}.

wave. While in the case of Au(bulk)–Mb(adsorbed) electrode, the oxidation peak potential is closer to 0.0 V *vs.* SCE, ($E_{pa} \approx 0.25$ V *vs.* SCE), in the case of Au(bulk)-MPS(−)/PDDA(+)/{HA/Mb}$_6$ the peak potential is shifted to more positive potentials at ≈+0.33 V *vs.* SCE.

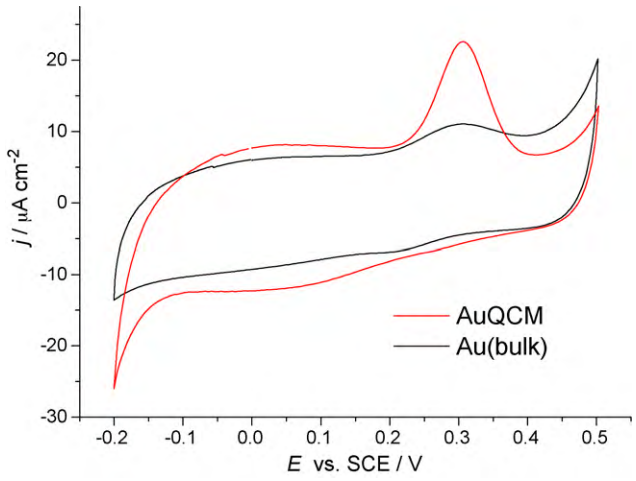

Fig. 8. Cyclic voltammograms at Au-MPS(−)/PDDA(+)/{HA/Mb}$_6$ in 0.05 M NaAcBS pH 5.0; scan rate 50 mV s^{-1}.

This is probably due to difficulties in electron transfer through the LBL structure, since the architecture is more complex, as discussed in more detail in Section 3.2.2, in which a decrease in the peak current was observed with an increase in the number of deposited layers. Therefore, the kinetics of electron transfer is also much faster in the case of Au(bulk)–Mb(adsorbed), the slope of the plots of I_{pa} *vs.* ν, being 0.115 μA cm^{-2} mV^{-1} s and 0.05 μA cm^{-2} mV^{-1} s for the AuQCM-MPS(−)/PDDA(+)/{HA/Mb}$_6$ (results not shown).

3.2.4. *Influence of pH on AuQCM- and Au(bulk)-modified electrodes*

The cyclic voltammetric response of AuQCM- and Au(bulk)-MPS(−)/PDDA(+)/{HA/Mb}$_6$ modified electrodes was recorded in 0.05 M NaAcBS solutions of different pH: 4.0, 4.7, 5.0, 5.3 and 5.7, going from pH 4.0 upto 5.7 and the opposite, as shown in Fig. 9. This pH range was chosen to ensure that HA and Mb are oppositely charged, since the isoelectric point of Mb (p*I* = 6.8) and pK_a of HA (pK_a = 2.9) have to be taken into account. The electrochemical response of the two different electrodes followed the same profile, with the difference that in the case of Au(bulk) modified electrodes, the recorded currents were lower, as already specified earlier. For both modified electrodes, it was observed that when experiments were first done in more acidic solution, pH 4.0, the oxidation peak current constantly decreased up to the highest pH of 5.7. When on the contrary, experiments were started at pH 5.7, the peak currents increased, reaching a maximum value at pH 5.0, then decreasing

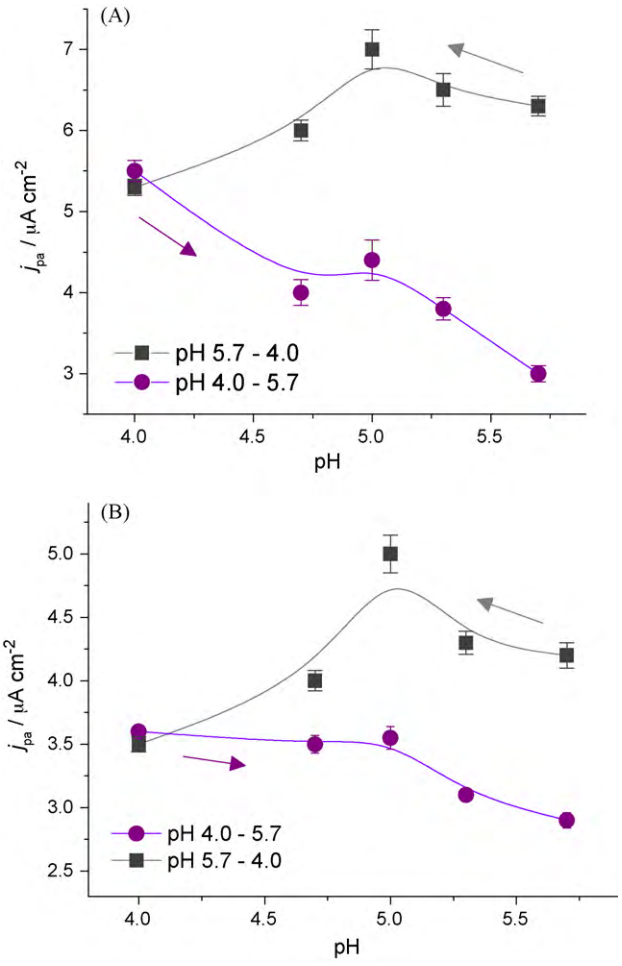

Fig. 9. Influence of pH on Au-MPS(−)/PDDA(+)/{HA/Mb}$_6$ modified electrode response (A) AuQCM and (B) Au(bulk); buffer solutions pH 4.0–5.7 are 0.05 M NaAcBS; scan rate 50 mV s^{-1}.

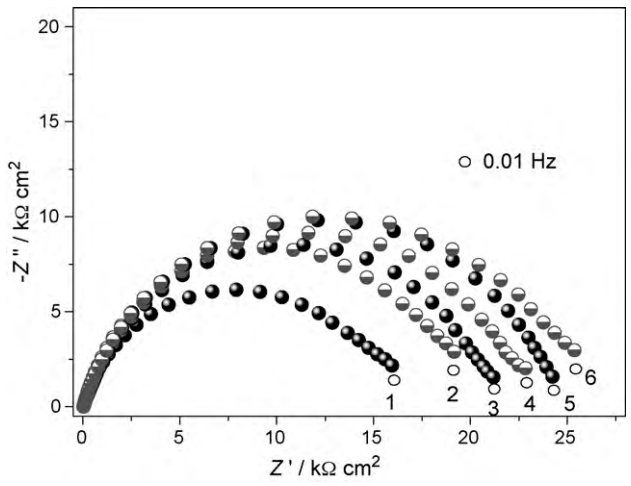

Fig. 10. Complex plane impedance plots spectra recorded at AuQCM-MPS(−)/PDDA(+)/{HA/Mb}$_{1-6}$ in 0.05 M NaAcBS solution pH 5.0 at OCP.

until pH 4.0. Probably the high concentration of protons in the solution of pH 4.0, leads to conformational changes of the protein with influence on the redox process. The optimal pH chosen for all further experiments was pH 5.0, at which the current response was the highest.

3.2.5. Stability of AuQCM-MPS(−)/PDDA(+)/{HA/Mb}$_6$

In order to evaluate the operational stability of the LBL films, the CV response was recorded during 100 scans, at 50 mV s^{-1} (data not shown). It was observed that the oxidation peak decreased 40% in size after the first 10 cycles, and then decreased only slightly up to the 100th cycle, reaching 50% of its initial value. Afterwards, another 50 cycles were recorded but no further decrease in peak current was observed. This initial decrease in response can be attributed to the loss of weakly adsorbed species at or near the electrode surface.

As mentioned above (Section 3.2.1), the storage stability was also evaluated by comparing the CV of a stabilised LBL-modified electrode (after an initial 10 cycles) kept in air, at room temperature. After 40 days of storage, the oxidation peak current decreased by only 10% from its initial value.

3.3. Electrochemical impedance spectroscopy

The electrical properties of the films during the layer-by-layer deposition of HA and Mb were also monitored by electrochemical impedance spectroscopy. Spectra shown in Fig. 10 were recorded in 0.05 M NaAcBS solution pH 5.0 at the open circuit potential (OCP), recorded before each EIS experiment.

The spectra were fitted to an equivalent electrical circuit, which consists of a cell resistance (R_Ω), in series with a charge transfer resistance (R_{ct}) in parallel with a constant phase element CPE = $\{(Ci\omega)^\alpha\}^{-1}$ to model a non-ideal capacitor, as done for other modified carbon electrodes e.g. [34,35]. The values of the α exponent obtained for AuQCM-MPS(−)/PPDA(+) was $\alpha = 0.89$, and an average value of $\alpha = 0.84$ was obtained for AuQCM-MPS(−)/PPD(+)/{HA/Mb}$_{1-6}$.

As seen, all spectra have a semicircular profile with the higher resistance in the case of AuQCM-MPS(−)/PDDA(+) of 160 kΩ cm^2, indicating a slow electron transfer. The R_{ct} value decreases substantially after the first {HA/Mb} bilayer deposition to 16 kΩ cm^2 and then starts to increase with each bilayer up to 28 kΩ cm^2 for the 6th bilayer. These substantially lower values are probably due to the presence of a free conductive species (heme) which, having a good mobility through the films, are able to reach the electrode surface, resulting in an increase in the amount of electron transfer at the interface.

The interfacial capacitance obtained was also the highest for AuQCM-MPS(−)/PPDA(+), $C = 82\ \mu F\ cm^{-2}$. At {HA/Mb}$_1$ modified electrode, the CPE value is smaller than at precursor modified electrode and continues to decrease up to the third bilayer, afterwards maintaining approximately the same value of $C_{dl} = 35\ \mu F\ cm^{-2}$.

The impedance spectra are in agreement with the cyclic voltammetry observations, which showed that the oxidation peak current decreases with deposition of each layer, corresponding to the observed increase in electron transfer resistance, and with the movement of free electroactive species. The combination of these techniques throws light on the electron transfer processes occurring in such systems.

4. Conclusion

The biocompatible hyaluronic acid and the heme protein, myoglobin have been successfully assembled onto Au electrode surfaces. Myoglobin, entrapped in LBL films with HA, exhibited a very stable, irreversible electrochemical response. Gravimetric measurements confirm an increase in the deposited mass with each layer, a total deposited mass being calculated of 18 μg cm^{-2}, with an average of 3 μg cm^{-2} per {HA/Mb} bilayer. Cyclic voltammetry showed that an electroactive species, other than Mb itself, but contained by it, attributed to free heme, is responsible for the electrochemical response. The oxidation peak recorded at ≈+0.3 V *vs.* SCE is very stable in time and is also observed at Au electrodes in Mb solution, the electrochemical behaviour being characteristic of electroactive thin films adsorbed at the electrode surface. EIS confirms the electroactivity of the films, the first {HA/Mb} bilayer exhibiting a higher charge transfer rate compared with the precursor MPS(−)/PDDA(+) modified electrode.

The LBL technique with the negative "hyaluronate" form of the polymer HA, can be applied for the immobilization of other oppositely charged biomolecules, enabling the inexpensive and easy construction of very stable films, with the use of very small amounts of enzyme or protein.

Acknowledgements

Financial support from Fundação para a Ciência e a Tecnologia (FCT), PTDC/QUI/65255/2006 and PTDC/QUI/65732/2006, POCI 2010 (co-financed by the European Community Fund FEDER) and CEMUC® (Research Unit 285), Portugal, is gratefully acknowledged. FCT is thanked for PhD grants for MMB (SFRH/BD/27864/2006) and EMP (SFRH/BD/31483/2006).

References

[1] F.A. Armstrong, J. Chem. Soc., Dalton Trans. 5 (2002) 661.
[2] Y. Wu, S. Hu, Microchim. Acta 159 (2007) 1.
[3] W. Schuhmann, Rev. Mol. Biol. 82 (2002) 425.
[4] F.A. Armstrong, G.S. Wilson, Electrochim. Acta 45 (2000) 2623.
[5] M. Lösche, Curr. Opin. Solid State Mater. Sci. 2 (1997) 546.
[6] G. Decher, Science 277 (1997) 1232.
[7] H. Ma, N. Hu, J.F. Rusling, Langmuir 16 (2000) 4969.
[8] G. Decher, J.B. Schlenoff, Multilayer Thin Films: Sequential Assembly of Nanocomposite Materials, Wiley–VCH, Weinheim, Germany, 2002.
[9] S.E. Burke, C.J. Barett, Biomacromolecules 4 (2003) 1773.
[10] D.L. Nelson, M.M. Cox, Lehninger Principles of Biochemistry, fifth ed., W.H. Freeman, USA, 2008.
[11] G. Wang, Y. Liu, N. Hu, Electrochim. Acta 53 (2007) 2071.
[12] W. Guo, N. Hu, Biophys. Chem. 129 (2007) 163.
[13] K. Qiao, H. Liu, N. Hu, Electrochim. Acta 53 (2008) 4654.
[14] Y. Xie, N. Hu, H. Liu, J. Electroanal. Chem. 630 (2009) 63.
[15] F. Caruso, K. Niiakura, D.N. Furlong, Y. Okahata, Langmuir 13 (1997) 3427.
[16] L. Lapčik Jr., L. Lapčik, Chem. Rev. 98 (1998) 2663.

[17] M.S. Lord, D. Pasqui, R. Barbucci, B.K. Milthorpe, Macromol. Symp. 266 (2008) 17.
[18] T.C. Laurent, J.R.E. Fraser, FASEB J. 6 (1992) 2397.
[19] S.E. Burke, C.J. Barett, Biomacromolecules 6 (2005) 1419.
[20] C. Picart, P. Lavalle, P. Hubert, F.J.G. Cuisinier, G. Decher, P. Schaaf, J.-C. Voegel, Langmuir 17 (2001) 7414.
[21] A. Szarpak, I. Pignot-Paintrand, C. Nicolas, C. Picart, R. Auzély-Velty, Langmuir 24 (2008) 9767.
[22] H. Lee, Y. Jeong, T.G. Park, Biomacromolecules 8 (2007) 3705.
[23] T.G. Kim, H. Lee, Y. Jang, T.G. Park, Biomacromolecules 10 (2009) 1532.
[24] T.I. Croll, A.J. O'Connor, G.W. Stevens, J.J. Cooper-White, Biomacromolecules 7 (2006) 1610.
[25] H. Lu, N. Hu, J. Phys. Chem. B 110 (2006) 23710.
[26] H. Lu, N. Hu, J. Phys. Chem. B 111 (2007) 1984.
[27] M.T. de Groot, M. Merkx, M.T.M. Koper, J. Am. Chem. Soc. 127 (2005) 16224.
[28] M.T. de Groot, M. Merkx, M.T.M. Koper, Electrochem. Commun. 8 (2006) 999.
[29] M.T. de Groot, M. Merkx, M.T.M. Koper, J. Biol. Inorg. Chem. 12 (2007) 761.
[30] G. Sauerbrey, Z. Phys. 155 (1959) 206.
[31] Y.M. Lvov, Z. Lu, J.B. Shenkmann, X. Zu, J.F. Rusling, J. Am. Chem. Soc. 120 (1998) 4073.
[32] C.C. Page, C.C. Moser, X. Chen, P.L. Dutton, Nature 402 (1999) 47.
[33] A. Bellelli, G. Antonini, M. Brunori, B.A. Springer, S.J. Sligar, J. Biol. Chem. 265 (1990) 18898.
[34] M.M. Barsan, E.M. Pinto, M. Florescu, C.M.A. Brett, Anal. Chim. Acta 635 (2009) 71.
[35] E.M. Pinto, C. Gouveia-Caridade, D.M. Soares, C.M.A. Brett, Appl. Surf. Sci. 255 (2009) 8084.